Measuring the Economic Value of Wind–Solar Complementarity in Europe Using Chance Constraints

Montree Jaidee[a], Bismark Singh[a,*]

[a]*School of Mathematical Sciences, University of Southampton, Southampton, SO17 1BJ, UK*

Abstract

The variability of wind and solar photovoltaic (PV) generation poses significant risks for producers in day-ahead electricity markets, where commitments must be made before actual output is realized. A common mitigation strategy is to invest in storage, but an alternative is to exploit the natural complementarity between wind and solar resources. We evaluate this economic value of cooperation using two stochastic optimization models with chance-constrained reliability guarantees: a Naive model without storage and a Storage-Enhanced model with battery dynamics. We evaluate the models using the European Meteorological derived High Resolution RES (EMHIRES) dataset for hourly wind and PV generation in 28 European countries in 2015. Our results show that cooperation consistently improves outcomes. Without storage, 24 of 28 countries achieve at least a 20% increase in expected profit, with gains in Finland, Lithuania, and Poland exceeding a seven-fold improvement. With storage included, absolute profits rise, but the relative advantage of cooperation becomes smaller and more uniform: joint profits are typically within 10–50% of the best independent operation. Cooperation remains most beneficial in countries like Belgium, Bulgaria, and the Netherlands, where wind and solar resources are both substantial and weakly negatively correlated. Methodologically, our work provides a demonstration of how chance-constrained optimization can evaluate renewable cooperation. For policymakers, our findings suggest that encouraging cooperative bidding can yield substantial and stable benefits in regions with balanced resources, whereas in resource-scarce settings, expanding capacity or scaling storage should take precedence.

Keywords: Chance-constrained optimization, Wind-solar complementarity, Battery storage, Renewable energy integration, European electricity markets

*Corresponding author

Email address: b.singh@southampton.ac.uk (Bismark Singh)

1. Introduction

The inherently intermittent nature of solar photovoltaic (PV) and wind power poses significant challenges for the reliable operation of electricity markets (Aflaki & Netessine, 2017; Glenk & Reichelstein, 2020; Piel et al., 2017). Solar output depends on diurnal and seasonal cycles, while wind generation is governed by complex meteorological dynamics that vary across space and time (Hu et al., 2015; Wolff et al., 2023). These fluctuations introduce risk in day-ahead electricity markets, where producers must commit to hourly energy deliveries before actual generation is realized. Failing to meet committed bids can result in financial penalties, reputational damage, or even the loss of future contracts (Sunar & Birge, 2019).

In operations and finance, a common strategy to manage uncertainty is to combine multiple sources of risk in a way that reduces overall exposure. This is especially effective when the uncertainties are negatively correlated or offer substitutable value. For example, in assortment planning, Kaut et al. (2021) show that pairing products with negatively correlated demand profiles can reduce the monetary portfolio risk. In financial hedging, Gaur & Seshadri (2005) illustrate how stock index options can protect against variable downturns when product demand is positively correlated with market performance. In manufacturing, Jordan & Graves (1995) demonstrate that process flexibility enables firms to shift capacity toward high-demand items, thus buffering against demand volatility across products. In all of these examples, the ability to combine or substitute across uncertain components reduces variance of the outcomes towards greater reliability.

This risk mitigation principle finds relevance to renewable energy systems as well. Wind and solar power exhibit partially complementary generation patterns — solar production peaks during daylight hours and declines at night, while wind power often intensifies in the evening or during non-summer months (we quantify this effect in Section 3). When these sources are negatively correlated, aggregating them can smooth total output and reduce the likelihood of simultaneous low generation. This complementarity has motivated the design of hybrid systems that co-locate wind and PV technologies (Ferrer-Martí et al., 2013; Golari et al., 2017; Salman et al., 2025), improving dispatchability and reducing backup requirements.

Recent studies have demonstrated both environmental and economic benefits of hybridizing wind and solar resources. For instance, Ferrer-Martí et al. (2013) formulate a mixed-integer program to co-optimize wind and PV in off-grid microgrids and report a 30.7% reduction in total capital cost. Golari et al. (2017) integrate intermittent renewable energy sources into a multi-plant, multi-stage production-inventory model and find that operational costs decrease by over 50% in a 12-stage single-plant setting and nearly 10% in a six-stage multi-plant setting. Their results also show that achieving a high green energy coefficient (the share of renewable energy in total energy consumption) is feasible and effective in reducing carbon footprint. Similarly, Atakan et al. (2022) use a stochastic hierarchical planning framework to manage the uncertainty introduced by wind and solar, showing that renewable integration can reduce generation costs by up to 10.4% and lower

daily CO_2 emissions. Glenk & Reichelstein (2020) analyze the investment value of hybrid wind and power-to-gas (P2G) systems, providing necessary and sufficient conditions under which joint deployment yields a synergistic benefit in terms of life-cycle unit costs. Empirical case studies further support these findings. In Urumqi, China, Li et al. (2013) show that hybrid wind–PV–battery systems reduce net present cost (NPC) by 9–11% relative to PV-battery and wind-battery systems. In Bangladesh, Nandi & Ghosh (2010) report even greater gains, with NPC reductions of 27% and 29% compared to wind-battery and PV-battery systems, respectively. Collectively, this extensive literature confirms that well-designed hybrid systems can significantly enhance the technical, economic, and environmental performance of renewable energy deployment.

Our work is in the same spirit as (Glenk & Reichelstein, 2020; Li et al., 2013; Nandi & Ghosh, 2010), but differs in focus and scope. Rather than evaluating investment decisions or long-term planning models, we study the operational coordination of a network of *independent* wind and solar producers in the context of the day-ahead electricity market. To model real-time delivery risk under uncertainty, we formulate stochastic optimization models with chance constraints, allowing a controlled probability of delivery shortfalls—an inherent feature of markets based on variable generation. A stochastic optimization framework is particularly well-suited for such an analysis, as it allows decision-making under uncertainty using simulations of scenario data. Further, chance constraints offer a flexible tool to enforce delivery reliability: operators can specify a desired confidence level (e.g., 95%) and ensure that energy commitments are met with high probability. This avoids the overly conservative behavior often associated with worst-case or deterministic models, while still providing reliability guarantees in uncertain environments. Employing this framework, we then quantify the economic benefits of joint operation and compare them to the profits from operating wind and solar assets independently. Our goal is to assess whether decentralized, market-based cooperation leads to measurable synergy, and to identify the operational conditions under which such cooperation is most effective.

With this background, the following are the key contributions of this work.

(i) We show that complementary generation profiles of wind and PV can substitute for storage. In many European regions, joint operation provides substantial synergy even without batteries — particularly in countries such as the Netherlands, the United Kingdom, and Germany where wind and solar outputs are negatively correlated — allowing natural complementarity to smooth delivery risk.

(ii) We find that although the value of cooperation is reduced when battery storage is introduced, it is not entirely eliminated. Storage tends to diminish the variability benefit of complementarity, shifting the advantage toward countries with more balanced or weakly correlated resources. In some cases, storage substitutes for cooperation, while in others it enhances synergy through temporal arbitrage.

(iii) We demonstrate that even without physical integration such as co-location or shared storage, simple coordination among independent operators generates significant economic gains. This suggests that market-based incentives for cooperative bidding can be as important as infrastructure investment.

(iv) Finally, at a methodological level, we present a case-study demonstrating that chance constraints provide a flexible tool for evaluating renewable energy cooperation. By varying the reliability threshold, we quantify how tolerant a system must be to delivery shortfalls in order for cooperation to remain profitable. This offers guidance for the calibration of imbalance penalties and reliability requirements in market design.

The rest of the article is structured as follows. Section 2 introduces the modeling framework and defines our surrogate measure for economic synergy. In Section 3 we summarize our dataset, provide an exploratory analysis of wind and solar generation across Europe, and outline the forecasting procedure that we use to generate our scenario sets. Section 4 reports the computational experiments and evaluates the performance of both models that we present, including sensitivity analyses with respect to battery capacity and reliability thresholds. Finally, Section 5 highlights the main insights and discusses their implications for renewable energy policy and market design.

2. Problem Setting

We study the economic value of cooperation between wind and solar producers participating in the day-ahead electricity market. The central question is whether these resources achieve higher profits when operating jointly rather than independently, and how this outcome depends on the presence of storage and on system reliability requirements. To capture the uncertainty of renewable generation, we employ chance-constrained optimization models that maximize expected profit while ensuring that committed hourly deliveries are met with high probability. The input to these models is a set of day-ahead forecast scenarios, generated from historical data as described in Section 3.2.

Our first framework, referred to as the *Naive* model, excludes storage and assumes that producers must commit to a fixed hourly delivery schedule before actual generation is realized. The model builds on the chance-constrained formulation in Singh et al. (2018), which analyzed the role of a fast-ramping generator in hedging renewable shortfalls. Let T denote the set of hours in the planning horizon, and let Ω denote the set of scenarios representing possible renewable generation outcomes. For each hour $t \in T$, the decision variable y_t denotes the committed delivery, while R_t represents the profit per unit of delivered energy. The available renewable generation in scenario $\omega \in \Omega$ is given by s_t^ω. The Naive model is formulated as

$$\max \quad \sum_{t \in T} R_t \, y_t \tag{1a}$$

$$\text{s.t.} \quad \mathbb{P}\left(y_t \leq s_t^\omega, \ \forall \, t \in T\right) \geq 1 - \varepsilon \tag{1b}$$

$$y_t \geq 0, \quad \forall\, t \in T. \tag{1c}$$

The chance constraint in (1b) is a *joint* reliability requirement over the full day: the entire vector of commitments $[y_t]_{t\in T}$ is covered by available generation $[s_t^\omega]_{t\in T}$ with probability at least $1-\varepsilon$. Equivalently, at most an ε fraction of possible day-ahead realizations may experience any shortfall at any hour. Smaller ε yields more conservative commitments and lower imbalance risk, while larger ε allows more aggressive bidding at the expense of occasional shortfalls. In our experiments we consider $\varepsilon \in \{0.01, 0.05\}$, corresponding to 99% and 95% daily reliability, respectively.

Building on this baseline model, the second framework extends the formulation by introducing a battery system that can charge and discharge to buffer renewable variability and improve delivery reliability. This *Storage-Enhanced* model is closely related to the chance-constrained approach in Singh & Knueven (2021), which studied the effect of battery integration for solar-based bidding. Let p_t^ω and q_t^ω denote the charge and discharge decisions, respectively, in hour t under scenario ω, and let x_t^ω denote the battery state of charge. The battery operates with round-trip efficiency η and is bounded between $\underline{X}$ and $\overline{X}$; charging and discharging incur per-unit costs C_c and C_d. The model is given by

$$\max \quad \sum_{t\in T} R_t\, y_t - \mathbb{E}\big[C_c\, p_t^\omega + C_d\, q_t^\omega\big] \tag{2a}$$

$$\text{s.t.} \quad \mathbb{P}\big(y_t \leq s_t^\omega + q_t^\omega - p_t^\omega,\ \forall\, t \in T\big) \ \geq\ 1-\varepsilon, \tag{2b}$$

$$x_{t+1}^\omega = x_t^\omega + \eta\, p_t^\omega - \tfrac{1}{\eta}\, q_t^\omega, \quad \forall\, t = 1, \ldots, |T|-1,\ \forall\, \omega \in \Omega, \tag{2c}$$

$$\underline{X} \leq x_t^\omega \leq \overline{X}, \quad \forall\, t \in T,\ \forall\, \omega \in \Omega, \tag{2d}$$

$$y_t,\ p_t^\omega,\ q_t^\omega \geq 0, \quad \forall\, t \in T,\ \forall\, \omega \in \Omega. \tag{2e}$$

In model (2), we apply the same joint reliability level $1-\varepsilon$ after accounting for storage. Further, the expectation in (2a) is taken with respect to the scenario distribution (implemented as a sample average approximation over Ω in our experiments). In optimal solutions of model (2), charging and discharging do not occur simultaneously (Singh & Knueven, 2021).

To implement the chance constraints in both models, we use a standard sample average approximation reformulation. Specifically, we introduce a binary variable z^ω for each scenario $\omega \in \Omega$, where $z^\omega = 1$ if the reliability constraint is violated in scenario ω. Then, each original chance constraint is replaced by scenario-specific linear constraints, augmented with a big-M term involving z^ω. Additionally, we enforce that at most $\lfloor N\varepsilon \rfloor$ violations occur across the $|\Omega|$ scenarios. This yields a mixed-integer linear program that we solve for each country and each reliability level.

We apply both models to three configurations: PV-only, wind-only, and joint wind–solar operation. Let z^{PV}, z^{W}, and z^{C} denote the optimal profits obtained by solving either (1) or (2) for

these cases. To evaluate the economic benefit of cooperation, we define the *Synergy Ratio* as

$$\mathrm{SR} \;=\; \frac{z^{\mathrm{C}}}{z^{\mathrm{W}} + z^{\mathrm{PV}}}. \tag{3}$$

A value of $\mathrm{SR} > 1$ indicates that joint operation of wind and solar achieves higher profit than the sum of independent operations, thereby quantifying the economic value of complementarity. This performance measure provides the link between the models and the computational analysis that we conduct in Section 3.

3. Data Description

3.1. Summary of Renewable Generation Data

We use the EMHIRES dataset (European Meteorologically derived High-resolution Renewable Energy Sources time series (Gonzalez Aparicio et al., 2016, 2017)) that provides hourly time series of onshore wind and PV generation across 35 European countries from January 1986 to December 2015. Each time series is reported as a *capacity factor* — the ratio of actual output in a given hour to the installed capacity — that takes values between zero and one. For this work, we focus on the year 2015 and restrict attention to the 28 countries for which complete capacity data and normalization parameters are available. Since our aim is to compare profitability across countries, we normalize the hourly capacity-factor profiles using the annual generation reported by each country's transmission system operator (TSO) for 2015. Multiplying the normalized capacity factors by installed capacities yields hourly generation in megawatts (MW), replicating each country's official annual production statistics. This normalization procedure is detailed in the appendix of Gonzalez Aparicio et al. (2016, 2017), and the final dataset used in our numerical experiments of Section 4 is available at our GitHub repository: `https://github.com/montreeklim/synergy_wind_solar`. In all tables and figures of this work, we identify countries by their ISO 3166-1 alpha-2 codes (e.g., DE = Germany, FR = France, etc.)

Table 1 summarizes the key descriptive statistics of hourly PV and wind generation across the 28 countries. For each technology, we report the mean, standard deviation, range (minimum and maximum), and the proportion of hours with zero output. We also calculate the PV share, defined as the ratio of average PV generation to the sum of average PV and wind generation, in order to characterize the balance between the two resources. The numbers show clear differences across the European countries. PV output follows a strict diurnal cycle, with nearly half of all hours producing zero output in most countries. Mean PV generation ranges from virtually zero in Ireland to nearly 4,000 MW in Germany. Wind generation, in contrast, is more continuous: in most countries, fewer than 5% of hours have zero output. Mean annual wind generation spans from below 1 MW in Slovenia and Slovakia to nearly 10,000 MW in Germany. The PV share is below 1% in northern

countries such as Estonia, Finland, Ireland, Norway, Poland, and Sweden, while exceeding 98% in Slovenia and Slovakia.

Table 1: Descriptive statistics of hourly PV and wind generation in 2015, derived from EMHIRES (Gonzalez Aparicio et al., 2016, 2017) and scaled to MW using country-level installed capacities reported by national transmission system operators (TSOs). The columns "Mean", "SD", "Range", and "%Z" denote the hourly mean, standard deviation, minimum–maximum range, and percentage of zero-output hours, respectively. The final column reports the PV share, defined as the ratio of average PV generation to the sum of average PV and wind generation. For details, see Section 3.1.

	PV (MW)				Wind (MW)				PV share (%)
Country	Mean	SD	Range	%Z	Mean	SD	Range	%Z	
AT	52.7	74.5	[0.0–287.6]	49.8	544.9	573.7	[0.0–1980.2]	0.0	8.8
BE	361.5	573.0	[0.0–2443.7]	49.9	503.2	504.7	[0.0–1726.0]	0.4	41.8
BG	152.1	226.4	[0.0–909.8]	49.4	118.8	126.5	[0.0–615.3]	0.1	56.1
CH	103.5	146.5	[0.0–551.1]	49.7	10.9	13.8	[0.0–60.0]	1.4	90.5
CZ	250.5	394.1	[0.0–1712.1]	49.4	67.1	74.7	[0.0–276.6]	0.6	78.9
DE	3922.2	5973.7	[0.0–25,535.6]	49.3	9670.2	10107.9	[10.4–42,757.6]	0.0	28.9
DK	83.0	135.7	[0.0–617.0]	49.6	999.7	844.9	[0.0–2837.1]	0.1	7.7
EE	0.5	1.0	[0.0–4.5]	50.6	77.8	65.2	[0.0–204.4]	0.4	0.6
ES	1220.1	1569.3	[0.0–5178.6]	49.5	5962.3	5054.0	[9.4–22,961.8]	0.0	17.0
FI	0.7	1.3	[0.0–6.3]	49.9	239.1	184.8	[0.7–679.8]	0.0	0.3
FR	828.1	1132.5	[0.0–4214.3]	49.9	2471.1	2031.9	[4.9–8683.0]	0.0	25.1
GB	853.2	1314.0	[0.0–6692.4]	49.3	4071.4	3031.0	[33.0–10,706.2]	0.0	17.3
GR	420.5	584.2	[0.0–2110.9]	49.8	375.1	349.0	[0.4–1517.5]	0.0	52.9
HR	5.8	8.9	[0.0–32.2]	49.4	65.4	83.2	[0.0–366.9]	4.4	8.1
HU	4.1	5.9	[0.0–21.1]	49.2	55.0	67.0	[0.0–263.4]	2.9	6.9
IE	0.1	0.1	[0.0–0.8]	49.7	759.9	583.3	[0.0–1759.9]	0.1	0.0
IT	2727.8	3819.8	[0.0–13,331.8]	49.6	1232.3	1396.9	[0.7–7444.8]	0.0	68.9
LT	6.7	11.5	[0.0–50.7]	50.3	67.1	66.9	[0.0–235.0]	0.4	9.1
LU	13.4	22.2	[0.0–95.6]	50.8	8.0	11.2	[0.0–48.4]	8.0	62.6
LV	0.2	0.3	[0.0–1.5]	50.2	12.0	11.9	[0.0–38.6]	2.7	1.6
NL	163.5	258.1	[0.0–1128.8]	49.9	972.4	850.1	[0.0–2594.1]	0.4	14.4
NO	0.7	1.3	[0.0–6.8]	49.2	209.5	124.5	[2.2–498.3]	0.0	0.3
PL	9.4	14.8	[0.0–66.2]	49.5	1324.5	1245.4	[1.2–4688.8]	0.0	0.7
PT	91.2	121.5	[0.0–388.4]	49.6	1073.9	968.5	[0.6–4506.3]	0.0	7.8
RO	178.0	250.9	[0.0–889.7]	49.6	579.7	568.3	[0.1–2859.6]	0.0	23.5
SE	7.8	13.1	[0.0–63.3]	49.5	937.4	752.5	[8.1–3018.3]	0.0	0.8
SI	32.2	51.6	[0.0–193.5]	50.1	0.4	0.7	[0.0–3.0]	17.5	98.8
SK	69.8	102.6	[0.0–383.8]	49.6	0.5	0.7	[0.0–2.6]	17.1	99.3

Figures 1a and 1b illustrate that in most countries average wind generation exceeds PV generation, with exceptions such as Italy, Greece, Bulgaria, the Czech Republic, and Switzerland. There are five countries (Ireland, Finland, Norway, Estonia, and Latvia) that have an average PV generation of less than 1 MW, and two countries (Slovenia and Slovakia) that have an average wind generation of less than 1 MW. Figure 1c and 1d further highlight the geographic distribution of resources: PV capacity is concentrated around the Mediterranean basin, where solar irradiance is high and sunshine is predictable, whereas wind capacity is concentrated in northwestern Europe, particularly Germany, the United Kingdom, and Spain, where strong and persistent wind regimes

prevail (we revisit this effect below). Finally, Figure 2 displays normalized hourly generation profiles, confirming the complementary temporal patterns of the two technologies: solar output peaks during daylight hours while wind generation tends to be stronger at night or during off-peak solar periods.

To examine complementarity more directly, we compute the Pearson correlation coefficient between hourly PV and wind generation during daytime hours (05:00–17:00). A negative correlation indicates that when one source produces strongly, the other tends to be weak, creating natural hedging opportunities; conversely, a positive correlation suggests that wind and solar outputs rise and fall together, offering less diversification benefit. As shown in Figure 3a, northern maritime countries such as Germany, the United Kingdom, and Norway exhibit strongly negative correlations in sunlit hours (as low as -0.55), reflecting a high degree of complementarity. In contrast, countries such as Hungary and Portugal display correlations closer to zero, implying weaker natural balancing.

To explore temporal patterns further, we group countries into four climatological regions: Atlantic Maritime, Continental, Nordic & Baltic, and Mediterranean. Figure 4 provides further details by plotting hourly PV–wind correlations for each climatological region. The Atlantic Maritime group (Figure 4a) shows the weakest negative correlation in the early morning [05:00–06:00), with correlations strengthening around 07:00–08:00 and then remaining relatively stable throughout the rest of the day. In the Mediterranean group (Figure 4d), correlations are also weak in the early morning but decrease steadily toward noon, reaching their most negative values late morning before increasing again in the afternoon; in Portugal, correlations even turn positive by 17:00. The Nordic & Baltic and Continental groups (Figures 4b and 4c) exhibit similar patterns, with the strongest negative correlations occurring around [06:00–07:00), rising toward weaker values near midday, and then becoming more negative again in the evening hours. These regional patterns reinforce the view that the degree of complementarity between PV and wind varies systematically not only across geography but also across the intraday cycle.

3.2. Scenario Generation

To evaluate the models introduced in Section 2, we simulate scenarios of renewable generation uncertainty at the day-ahead horizon. Specifically, we use an autoregressive moving average (ARMA) model following the methodology given in Singh & Pozo (2019).

For wind generation, we fit an ARMA(p, q) model to the 60 days of data preceding the prediction date of September 28, 2015 (the 271st day of the year). We verify stationarity using the Augmented Dickey–Fuller (ADF) test, with the null hypothesis of a unit root rejected at the 5% level in all countries. We evaluate candidate lag orders $p, q \in \{0, \ldots, 5\}$ to select the model that minimizes the Bayesian Information Criterion (BIC), subject to passing Ljung–Box tests for residual autocorrelation at lags 5, 10, and 15. For four countries (Bulgaria, France, Greece, and Romania), no specification satisfies all Ljung–Box tests; in these cases, we select the model with minimum BIC, as our goal is scenario generation rather than best-in-class forecasting accuracy.

Figure 1: Average hourly wind and PV generation by country in 2015 (MW), shown on a logarithmic scale to accommodate cross-country magnitude differences, based on EMHIRES data (Gonzalez Aparicio et al., 2016, 2017). For details, see Section 3.

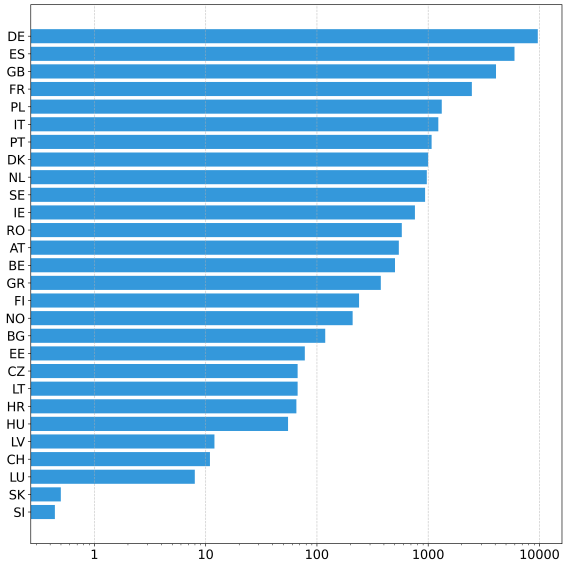

(a) Average hourly wind generation (bar chart).

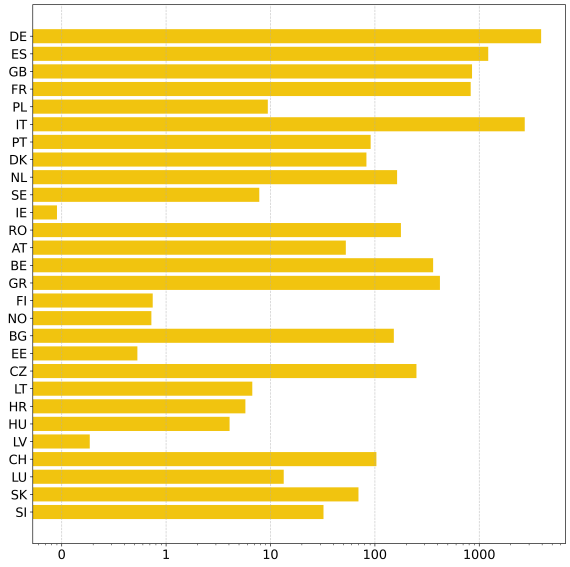

(b) Average hourly PV generation (bar chart).

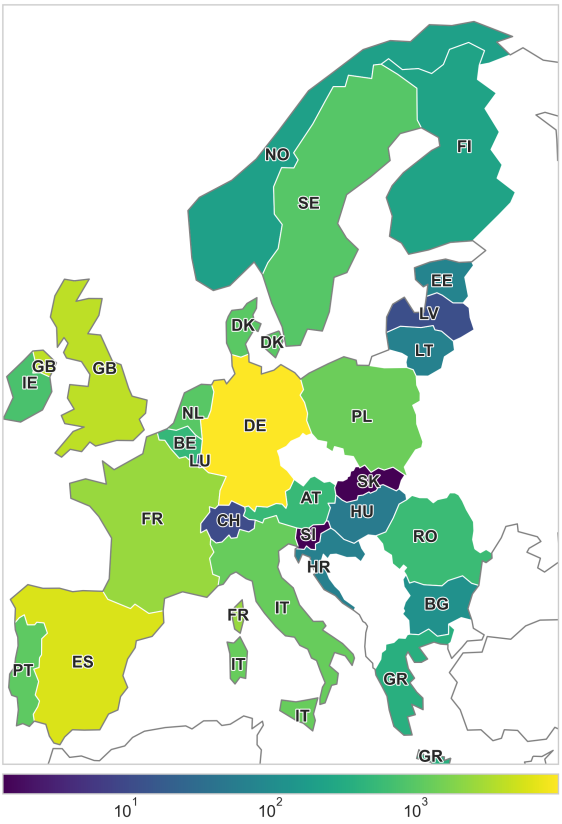

(c) Average hourly wind generation (heatmap).

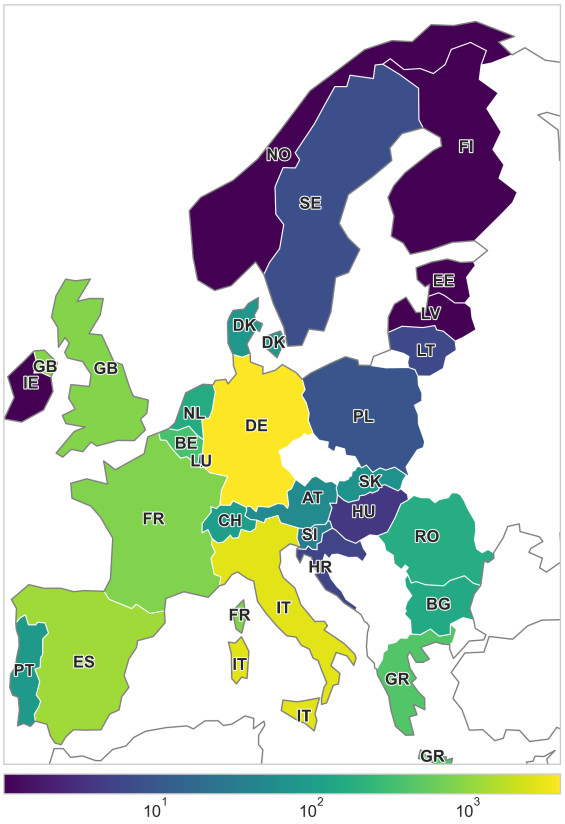

(d) Average hourly PV generation (heatmap).

Figure 2: Intraday generation profiles of PV (orange), wind (blue), and their sum (green) for 28 European countries normalized by that country's peak combined hourly output. The x-axis denotes the hour of the day ranging from 0:00 to 23:00, while the y-axis provides the corresponding value. Data is based on the 2015 EMHIRES data (Gonzalez Aparicio et al., 2016, 2017). See Section 3 for details.

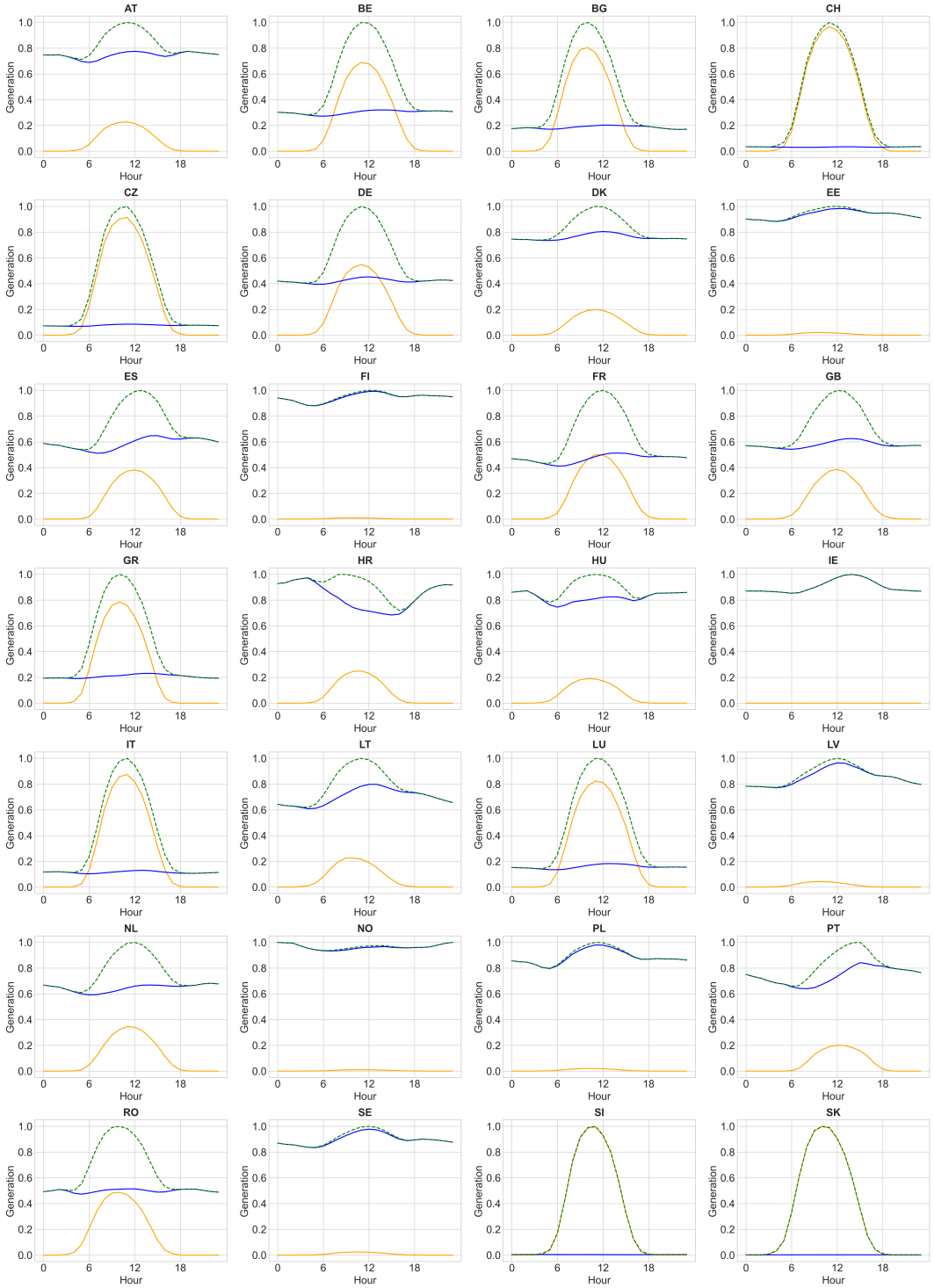

Figure 3: Spatial patterns of PV–wind correlation and climatological regionalization based on EMHIRES data (Gonzalez Aparicio et al., 2016, 2017). Daytime hours are defined as 05:00–17:00. For details, see Section 3.

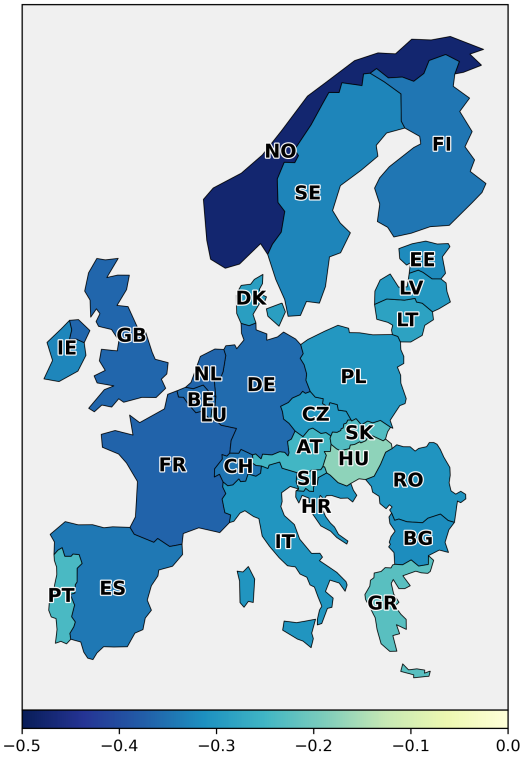

(a) Average hourly PV–wind correlation by country (daytime hours).

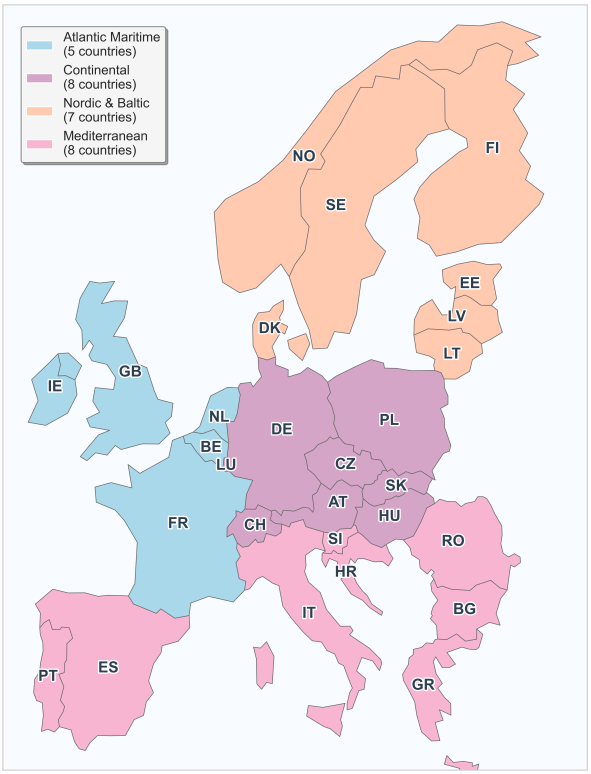

(b) European countries grouped by climate regions.

Figure 4: Hourly PV–wind correlation profiles for European countries, grouped by climatological region. The underlying data is from the 2015 EMHIRES dataset Gonzalez Aparicio et al. (2016, 2017). Colored lines represent countries within the focal region, while all other countries appear in gray. See Section 3 for details.

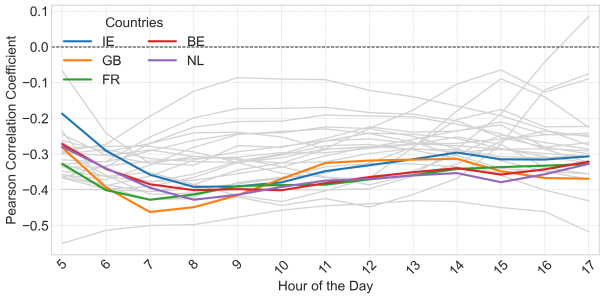

(a) Atlantic Maritime

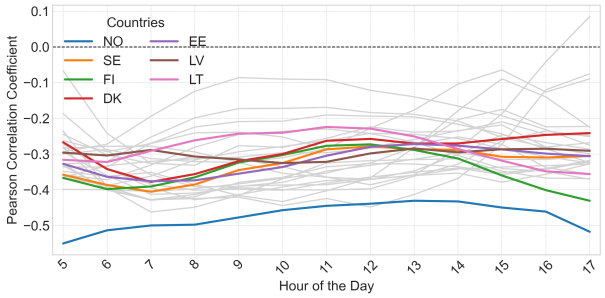

(b) Nordic & Baltic

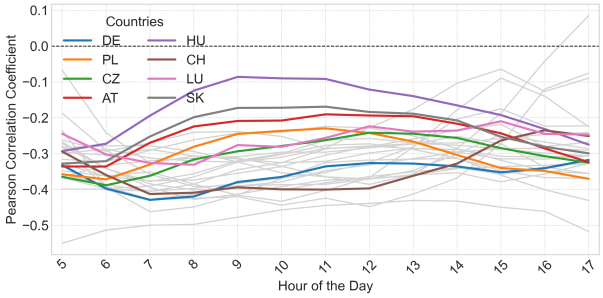

(c) Continental

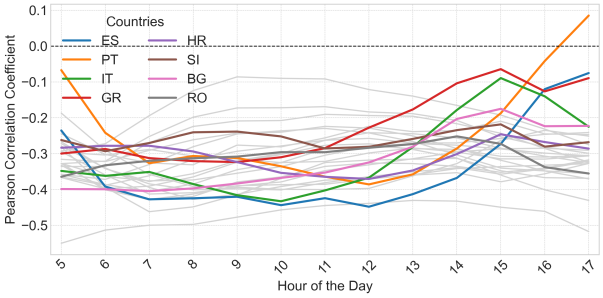

(d) Mediterranean

For PV generation, we fit separate ARMA models for each hour of the day, using the 270 days preceding September 28, 2015. For hours where output was zero in the previous seven days, we directly predict zero generation. We again verify stationarity with the ADF test, and difference the non-stationary series until stationarity is achieved. We then estimate ARMA(p, q) models with $p, q \in \{0, \ldots, 5\}$ and select lag orders using BIC, ensuring residuals do not exhibit significant autocorrelation. For differenced series, we transform back the forecast values by adding the last observed level of the original series.

Using these fitted models, we generate 10 independent batches of 100 Monte Carlo scenarios for each country and technology. Each scenario represents a 24-hour trajectory of possible generation outcomes, truncated below at zero. For illustration, Figures 5a and 5b provide a representative set of 100 scenarios for the United Kingdom, with black lines indicating the 10th percentile, median, and 90th percentile. These scenarios capture the variability and uncertainty inherent in renewable generation and provide the basis for evaluating the performance of the Naive and Storage-Enhanced optimization models in Section 4.

Figure 5: Illustrative set of 100 hourly scenarios for renewable generation in the United Kingdom derived from ARMA models. The panels show (a) wind power and (b) solar PV output; dashed black lines indicate the median and solid black lines the 10th percentile across scenarios. For details, see Section 3.2.

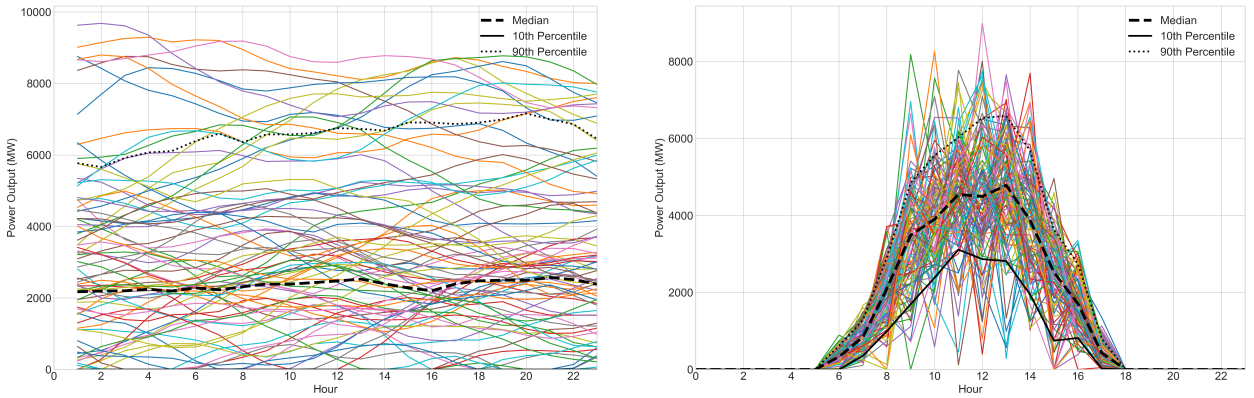

(a) Wind generation

(b) PV generation

4. Computational Experiments

In this section, we present numerical experiments conducted using the models described in Section 2. The input consists of hourly wind and solar generation scenarios derived from the EMHIRES dataset (Section 3). For each of the 28 countries, we evaluate both the Naive and Storage-Enhanced models under reliability levels $1 - \varepsilon \in \{0.95, 0.99\}$, with 10 independent sets of 100 scenarios each. We run all computational experiments on a computing cluster with an Intel Xeon Gold 6138 2.0 GHz processor, 192 GB of RAM, and Gurobi 10.0.3 via Python 3.8.3. Each instance has a time limit of one hour.

We present our analysis in three parts. In Section 4.1, we first report results for the Naive model, highlighting the value of complementarity in the absence of storage. Section 4.2 examines how battery integration alters profits and synergy patterns. Section 4.3 presents sensitivity analyses with respect to storage capacity and reliability thresholds. Throughout, we interpret results in terms of the Synergy Ratio, defined in equation (3), which serves as our measure of the economic value of cooperation.

4.1. Analysis of the Naive Model: No Storage

Table 2 presents the 95% confidence intervals for the Synergy Ratio; our numbers exclude experiments where the synergy ratio is undefined. Under the Naive model (columns 2–3), requiring strict reliability ($\varepsilon = 0.01$) produces an undefined ratio in the Czech Republic, Estonia, Finland, Lithuania, Latvia, and Slovenia due to zero profits in both individual sources but a positive value for combined sources. Omitting these degenerate cases, Poland and Croatia have the highest Synergy Ratio with confidence intervals of $(14.27, 31.01)$ and $(1.77, 31.64)$, respectively. Slovakia has the smallest profit gains with a confidence interval of $(1.02, 1.07)$. Overall, the minimum ratio for all countries is greater than one, which indicates that combining wind and PV generation provides more profit than individual operation. However, we note that this ratio is highly dependent on the generated scenarios, e.g., in Ireland with $\varepsilon = 0.01$, the confidence interval range is between -8.20 to 139.29 with a negative lower bound value due to the large standard deviation. With the reliability threshold of $\varepsilon = 0.01$, the results are not strongly conclusive due to the relatively wide confidence intervals.

Relaxing the reliability threshold to $\varepsilon = 0.05$, narrows the confidence interval considerably suggesting more precise estimates. Specifically, the lower bounds fall into the tighter range of 0.99 to 8.85, while the upper bounds range from 1.02 to 30.54. This contraction occurs because allowing more scenario violations raises the minimum objective values, thereby reducing cases in which the profit from one resource is nearly zero. As a result, the relative gains from cooperation become more stable and easier to compare across countries, with less dependence on individual scenario variation. In this setting, the largest gains occur in Finland, Lithuania, and Poland, where joint operation yields at least 7.5 times the profit of independent wind or solar systems. By contrast, the lowest ratios remain in Latvia, Norway, Slovenia, and Slovakia, where values hover just above one indicating only marginal improvement over independent operation. Notably, Norway and Latvia have PV shares below two percent, while Slovenia and Slovakia have PV shares exceeding 98%. This pattern suggests that when one resource contributes only a negligible share of total generation, cooperation may not yield meaningful additional value.

Table 2: 95% confidence intervals defined over 10 samples for the Synergy Ratio, see equation (3), for 28 European countries for both the Naive and Storage-Enhanced models. Entries with "–" indicates that the synergy ratio is undefined for at least nine out of the 10 samples due to zero profits from both wind and PV generation sources but non-zero profits from the combination. For details, see Section 4.1.

Country	**Naive**		**Storage-Enhanced**	
	$\varepsilon = 0.01$	$\varepsilon = 0.05$	$\varepsilon = 0.01$	$\varepsilon = 0.05$
AT	(2.66, 8.02)	(3.05, 4.39)	(1.30, 1.39)	(1.18, 1.29)
BE	(3.76, 7.32)	(3.03, 4.04)	(1.30, 1.38)	(1.30, 1.38)
BG	(1.75, 3.49)	(1.58, 1.97)	(1.25, 1.36)	(1.29, 1.43)
CH	(1.43, 3.39)	(1.27, 1.39)	(1.06, 1.09)	(1.08, 1.10)
CZ	(–, –)	(1.40, 1.78)	(1.14, 1.21)	(1.15, 1.18)
DE	(1.51, 1.99)	(1.60, 1.96)	(1.19, 1.28)	(1.27, 1.36)
DK	(2.88, 3.88)	(2.70, 3.57)	(1.21, 1.28)	(1.24, 1.30)
EE	(–, –)	(2.77, 4.94)	(1.05, 1.08)	(1.04, 1.07)
ES	(1.26, 1.38)	(1.31, 1.42)	(1.14, 1.19)	(1.14, 1.20)
FI	(–, –)	(7.75, 16.38)	(1.02, 1.03)	(1.02, 1.03)
FR	(1.69, 2.09)	(1.72, 1.98)	(1.22, 1.27)	(1.20, 1.27)
GB	(2.16, 3.04)	(2.01, 2.40)	(1.25, 1.31)	(1.21, 1.28)
GR	(1.33, 1.45)	(1.31, 1.41)	(1.18, 1.23)	(1.20, 1.24)
HR	(1.77, 31.64)	(4.08, 6.34)	(1.17, 1.21)	(1.23, 1.27)
HU	(1.66, 9.76)	(2.57, 3.53)	(1.16, 1.20)	(1.18, 1.26)
IE	(-8.20, 139.29)	(1.78, 4.22)	(1.00, 1.00)	(1.00, 1.00)
IT	(1.25, 1.40)	(1.23, 1.33)	(1.12, 1.16)	(1.12, 1.16)
LT	(–, –)	(8.85, 30.54)	(1.36, 1.46)	(1.29, 1.42)
LU	(2.19, 8.09)	(2.22, 3.31)	(1.23, 1.35)	(1.27, 1.35)
LV	(–, –)	(0.99, 1.52)	(1.07, 1.10)	(1.07, 1.10)
NL	(3.10, 4.33)	(3.05, 3.94)	(1.39, 1.51)	(1.29, 1.39)
NO	(2.50, 8.12)	(1.05, 1.17)	(1.01, 1.04)	(1.01, 1.01)
PL	(14.27, 31.01)	(7.64, 10.62)	(1.05, 1.06)	(1.03, 1.05)
PT	(1.39, 1.60)	(1.40, 1.55)	(1.12, 1.20)	(1.05, 1.09)
RO	(-0.13, 11.03)	(2.20, 3.86)	(1.31, 1.42)	(1.31, 1.44)
SE	(2.49, 4.81)	(2.35, 4.03)	(1.07, 1.10)	(1.06, 1.09)
SI	(–, –)	(1.02, 1.06)	(1.01, 1.02)	(1.01, 1.02)
SK	(1.02, 1.07)	(1.01, 1.02)	(1.00, 1.01)	(1.01, 1.01)

4.2. Analysis of the Storage-Enhanced Model: With Storage

Table 2 (columns 4–5) reports the 95% confidence intervals for the Synergy Ratio under the Storage-Enhanced model with battery capacity set equal to the installed capacity for each resource (i.e., the maximum generation in an hour). In contrast to the Naive model, all countries yield defined ratios in this setting because the presence of a battery ensures strictly positive profits for both wind-only and PV-only operations, even under the stringent reliability requirement of $\varepsilon = 0.01$. As a result, the confidence intervals are markedly tighter and extreme values disappear.

For $\varepsilon = 0.01$, the lower bounds range from 1.00 (Ireland) to 1.39 (the Netherlands), while the upper bounds range from 1.00 (Ireland) to 1.51 (the Netherlands). Relaxing the threshold to $\varepsilon = 0.05$ yields a very similar pattern, with lower bounds between 1.00 and 1.31 and upper bounds between 1.00 and 1.44. This stability across reliability levels reflects how storage dampens the sensitivity of profits to forecast uncertainty.

However, the presence of storage reduces the Synergy Ratio in most countries. For example, Finland and Poland, which achieved Synergy Ratios well above seven in the Naive model, fall below 1.06 under the Storage-Enhanced model. The reason is that when one resource is scarce (e.g., PV in northern regions or wind in Slovenia and Slovakia), the battery substitutes for the missing complementarity, leaving little additional benefit from cooperation. In these cases, the ratio drops close to one, indicating that joint operation does not improve profit relative to independent participation significantly. Despite this, several countries retain Synergy Ratios above 1.25 even with storage. Belgium, Bulgaria, Lithuania, the Netherlands, and Romania all lie in this category, with ratios between 1.25 and 1.51. The presence of storage in these regions enhances the ability to exploit temporal arbitrage opportunities, allowing cooperation to remain economically beneficial. In countries with strongly complementary profiles (e.g., France, the Netherlands, the United Kingdom, Germany), Synergy Ratios are much lower compared to the Naive model and tend to decrease further as battery capacity increases, indicating that storage substitutes for natural balancing of renewable generation, see Section 4.3.

There are country-specific caveats in the above analysis. While Norway exhibits one of the most strongly negative PV–wind correlations, its Synergy Ratio remains low. In other words, even though PV and wind in Norway tend to alternate (i.e., high wind when solar is low, and vice versa), the economic gain from combining them is negligible because Norwegian solar output is extremely small compared to wind. This interpretation is reinforced by the cases of Slovenia and Slovakia (where the PV share is more than 98%), and by Finland, Ireland, and Norway (where the PV share is less than 0.5%). In each of these cases, the scarcity of one resource limits the potential for meaningful synergy. Similarly, the ratio for Ireland is not high, even though it shares correlation patterns with high-SR countries because its PV share is very low.

Summarizing, our results lead to two takeaways. First, storage systematically increases total profits, but it also reduces the incremental value of natural complementarity in highly correlated systems by providing an alternative buffer against variability. In these cases, storage acts as a substitute for the natural balancing between wind and solar. As capacity grows the incremental benefit of cooperation diminishes further. Second, the relative ordering of countries by Synergy Ratio remains stable across reliability thresholds, highlighting that the economic role of storage is not to eliminate complementarity, but to redistribute its value across regions with different resource profiles.

4.3. Sensitivity Analysis

Next, we examine how the value of cooperation depends on three factors: battery capacity, reliability thresholds, and the correlation between wind and solar generation. We also report average profit outcomes to properly place the Synergy Ratios in an economic context.

In the Storage-Enhanced model (2), the battery frequently serves as the primary instrument for arbitraging across hours with pronounced price differences. For instance, in several countries the optimal policy at hour 17:00 is to discharge the battery to its lower bound as the market return during that hour outweighs the cycling cost. This pattern suggests that benchmarking battery size to the installed renewable capacity of each setting may understate the potential benefits of cooperation. To investigate this effect, we re-ran the combined-system experiments on a dataset different from that used in Table 2, varying battery capacity to be either one-half or twice the installed capacity in each case.

Table 3 shows that reducing battery capacity markedly increases Synergy Ratios. With capacity set to one-half of installed capacity, confidence intervals widen for most countries, reflecting greater variability. Under $\varepsilon = 0.01$, Lithuania, the Netherlands, and Romania attain the highest Synergy Ratios, each reaching at least 1.47. Under $\varepsilon = 0.05$, Lithuania, Romania, and Belgium again lead with ratios of at least 1.40. By contrast, Finland, Ireland, Norway, Slovakia, and Slovenia record the lowest ratios converging to 1.00 across all battery sizes. This suggests that in these regions the Storage-Enhanced model offers little advantage over independent wind–battery and PV–battery systems. Doubling battery capacity produces the opposite effect: Synergy Ratios decline but become more stable, with narrower confidence intervals. Thus, smaller storage capacities raise the measured value of wind–solar complementarity, as cooperation compensates for the reduced buffering from storage, but this comes at the cost of wider uncertainty ranges. In extreme cases, further reducing capacity could replicate the volatility observed in the Naive model.

Sensitivity to the reliability parameter ε is much less pronounced in the Storage-Enhanced model than in the Naive model. Table 2 shows that relaxing the reliability requirement from $\varepsilon = 0.01$ to $\varepsilon = 0.05$ substantially narrows the confidence intervals in the Naive model (e.g., Poland from (14.27, 31.01) to (7.64, 10.62); Ireland from $(-8.20, 139.29)$ to (1.78, 4.22)). This contraction reflects the fact that higher tolerance reduces the frequency of near-zero denominators in the ratio. By contrast, confidence intervals under the Storage-Enhanced model change little between the two thresholds (e.g., Romania (1.31, 1.42) to (1.31, 1.44); Lithuania (1.36, 1.46) to (1.29, 1.42)). These results confirm that storage buffers against variability not only in generation but also in the sensitivity of cooperative value to reliability requirements.

Figure 6a illustrates that the box plot for the Synergy Ratio in the Naive model has a wider box for $\varepsilon = 0.01$ than for $\varepsilon = 0.05$ across all regions, except for the Nordic & Baltic region. In the latter, four of the six countries with an undefined ratio are excluded from the plot. The Nordic & Baltic region has the longest interquartile range and the highest median Synergy Ratio, whereas

Table 3: Synergy Ratios, see equation (3), for 28 European countries under different battery capacities, for two reliability levels of 95% ($\varepsilon = 0.05$) and 99% ($\varepsilon = 0.01$). The Baseline column denotes the default battery size, while the Half Cap. and Double Cap. columns denote a battery size of half and double the installed capacity. For details, see Section 4.3.

Country	$\varepsilon = 0.01$			$\varepsilon = 0.05$		
	Half Cap.	Baseline	Double Cap.	Half Cap.	Baseline	Double Cap.
AT	(1.50, 1.62)	(1.30, 1.39)	(1.17, 1.22)	(1.21, 1.40)	(1.18, 1.29)	(1.12, 1.18)
BE	(1.44, 1.53)	(1.30, 1.38)	(1.21, 1.28)	(1.42, 1.51)	(1.30, 1.38)	(1.23, 1.29)
BG	(1.44, 1.55)	(1.25, 1.36)	(1.15, 1.24)	(1.45, 1.57)	(1.29, 1.43)	(1.19, 1.31)
CH	(1.10, 1.12)	(1.06, 1.09)	(1.05, 1.08)	(1.11, 1.13)	(1.08, 1.10)	(1.06, 1.08)
CZ	(1.22, 1.26)	(1.14, 1.21)	(1.11, 1.16)	(1.21, 1.27)	(1.15, 1.18)	(1.11, 1.14)
DE	(1.29, 1.41)	(1.19, 1.28)	(1.13, 1.20)	(1.36, 1.44)	(1.27, 1.36)	(1.19, 1.26)
DK	(1.39, 1.49)	(1.21, 1.28)	(1.12, 1.16)	(1.35, 1.47)	(1.24, 1.30)	(1.15, 1.18)
EE	(1.11, 1.16)	(1.05, 1.08)	(1.03, 1.04)	(1.06, 1.13)	(1.04, 1.07)	(1.02, 1.03)
ES	(1.20, 1.24)	(1.14, 1.19)	(1.09, 1.13)	(1.18, 1.24)	(1.14, 1.20)	(1.09, 1.14)
FI	(1.04, 1.06)	(1.02, 1.03)	(1.01, 1.02)	(1.03, 1.06)	(1.02, 1.03)	(1.01, 1.02)
FR	(1.30, 1.35)	(1.22, 1.27)	(1.15, 1.19)	(1.27, 1.33)	(1.20, 1.27)	(1.15, 1.20)
GC	(1.23, 1.28)	(1.18, 1.23)	(1.14, 1.18)	(1.24, 1.28)	(1.20, 1.24)	(1.16, 1.20)
HR	(1.36, 1.43)	(1.17, 1.21)	(1.09, 1.12)	(1.43, 1.50)	(1.23, 1.27)	(1.13, 1.15)
HU	(1.34, 1.42)	(1.16, 1.20)	(1.08, 1.11)	(1.30, 1.47)	(1.18, 1.26)	(1.10, 1.14)
IE	(1.00, 1.00)	(1.00, 1.00)	(1.00, 1.00)	(1.00, 1.00)	(1.00, 1.00)	(1.00, 1.00)
IT	(1.16, 1.20)	(1.12, 1.16)	(1.09, 1.13)	(1.14, 1.19)	(1.12, 1.16)	(1.10, 1.13)
LT	(1.60, 1.76)	(1.36, 1.46)	(1.21, 1.27)	(1.40, 1.67)	(1.29, 1.42)	(1.19, 1.25)
LU	(1.33, 1.47)	(1.23, 1.35)	(1.16, 1.26)	(1.35, 1.46)	(1.27, 1.35)	(1.19, 1.26)
LV	(1.14, 1.20)	(1.07, 1.10)	(1.03, 1.05)	(1.12, 1.18)	(1.07, 1.10)	(1.04, 1.05)
NL	(1.61, 1.76)	(1.39, 1.51)	(1.25, 1.33)	(1.38, 1.53)	(1.29, 1.39)	(1.21, 1.27)
NO	(1.02, 1.06)	(1.01, 1.04)	(1.01, 1.02)	(1.01, 1.02)	(1.01, 1.01)	(1.00, 1.01)
PL	(1.10, 1.13)	(1.05, 1.06)	(1.02, 1.03)	(1.04, 1.09)	(1.03, 1.05)	(1.02, 1.02)
PT	(1.20, 1.33)	(1.12, 1.20)	(1.07, 1.12)	(1.08, 1.14)	(1.05, 1.09)	(1.04, 1.06)
RO	(1.47, 1.67)	(1.31, 1.42)	(1.18, 1.24)	(1.46, 1.68)	(1.31, 1.44)	(1.19, 1.27)
SI	(1.02, 1.04)	(1.01, 1.02)	(1.01, 1.02)	(1.02, 1.03)	(1.01, 1.02)	(1.01, 1.02)
SK	(1.01, 1.02)	(1.00, 1.01)	(1.00, 1.01)	(1.01, 1.01)	(1.01, 1.01)	(1.00, 1.01)
SE	(1.15, 1.20)	(1.07, 1.10)	(1.04, 1.05)	(1.10, 1.17)	(1.06, 1.09)	(1.03, 1.05)
GB	(1.38, 1.45)	(1.25, 1.31)	(1.18, 1.22)	(1.29, 1.39)	(1.21, 1.28)	(1.17, 1.21)

Figure 6: Synergy Ratio distributions by climatological region. The left panel shows box plots for the Naive model, and the right panel shows box plots for the Storage-Enhanced model. Both figures have different scales. For details, see Section 4.3.

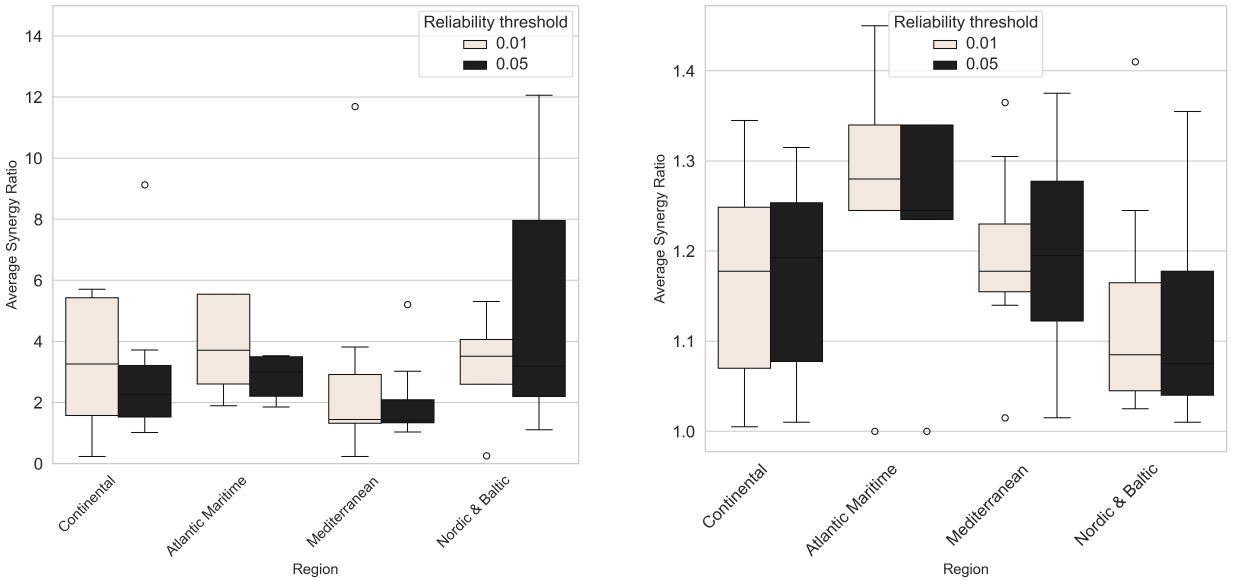

(a) Naive model.

(b) Storage-Enhanced model.

the Mediterranean region has the lowest values for both these measures. In the Storage-Enhanced model shown in Figure 6b, the difference in the box length between $\varepsilon = 0.01$ and $\varepsilon = 0.05$ is lesser compared to Figure 6a. The Atlantic Maritime region has the highest median for both of these reliability thresholds, whereas the Nordic & Baltic region has the lowest, despite having the highest median in the Naive model.

Figure 7 presents the relationship between PV–wind correlation and the average Synergy Ratio under the Storage-Enhanced model across three periods of the day. Correlation in the early morning is measured from 05:00 to 07:00, daytime from 07:00 to 16:00, and late afternoon from 16:00 to 18:00. We exclude countries with PV shares below 0.5% or above 95% since extreme scarcity of one resource renders cooperation uninformative. Fitted regressions yield $R^2 = 0.39$ for $\varepsilon = 0.01$ and $R^2 = 0.32$ for $\varepsilon = 0.05$ in the late afternoon period, suggesting a weak but nontrivial association: more negative correlations in the late afternoon are coinciding with higher synergy. This pattern aligns with the intuition that complementarity is strongest when solar output declines sharply while wind availability offsets the shortfall. By contrast, no meaningful relationship between correlation and synergy is observed in the early morning or daytime periods.

Finally, Table 4 reports average profits for each country under both models. As expected, storage increases absolute profits in every case. The relative gains are very large in countries with near-zero baseline profits in the Naive model (e.g., Estonia, Finland, Ireland, Latvia, Slovenia,), but these numbers are inflated by the small denominators. By contrast, in larger systems with

Figure 7: PV-wind correlation in each period versus average Synergy Ratio in the Storage-Enhanced model, excluding countries with a PV share below 0.5% or above 98%. Shaded bands denote 95% confidence intervals for the fitted regression lines.

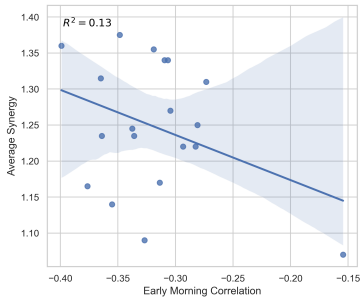

(a) Early Morning ($\epsilon = 0.01$)

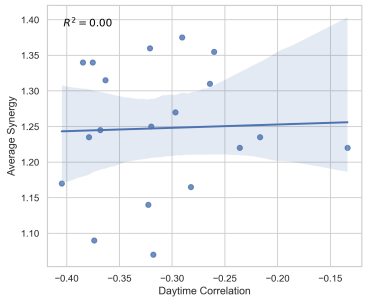

(b) Daytime ($\epsilon = 0.01$)

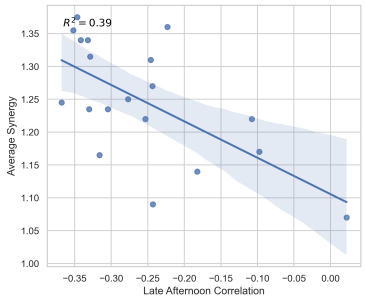

(c) Late Afternoon ($\epsilon = 0.01$)

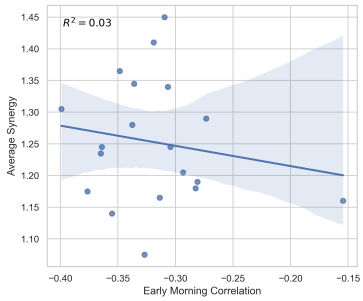

(d) Early Morning ($\epsilon = 0.05$)

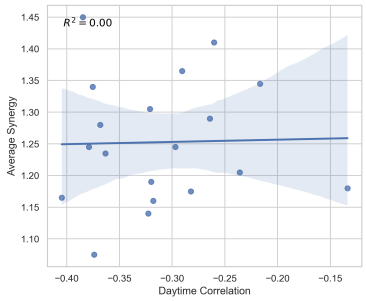

(e) Daytime ($\epsilon = 0.05$)

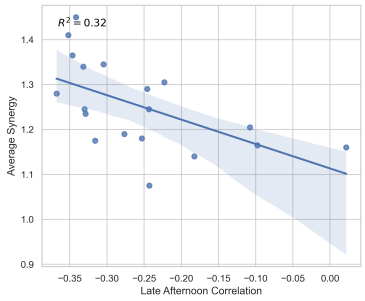

(f) Late Afternoon ($\epsilon = 0.05$)

substantial renewable capacity (France, Greece, Italy, the United Kingdom), storage delivers more modest percentage gains (about 110–280%) yet translates into absolute increases of several hundred thousand euros. In other words, while small systems exhibit dramatic percentage improvements, the most significant economic benefits in absolute terms accrue to the larger countries.

Summarizing this sensitivity analysis, three patterns emerge. First, increasing battery capacity raises absolute profits but reduces the incremental value of cooperation, particularly in resource-scarce or strongly complementary systems where storage substitutes for natural balancing. Second, storage stabilizes outcomes by reducing the sensitivity of Synergy Ratios to reliability thresholds thereby providing more predictable cooperative benefits. Third, correlations matter, but only partially: while negative PV-wind correlation in the late afternoon tends to support higher synergy, other temporal and operational factors play an equally important role. Taken together, these findings highlight that the economic value of cooperation is not determined by complementarity alone, but also by its interaction with storage capacity and broader system design.

Table 4: Average profits (in thousands of US dollars) from the combined wind and PV system under the Naive and Storage-Enhanced models for two reliability levels, $\varepsilon \in \{0.01, 0.05\}$. The ratios in parentheses show the multiplicative increase in profit from the Naive to the Storage-Enhanced model. For details, see Section 4.3.

Country	**Naive**		**Storage-Enhanced**	
	$\varepsilon = 0.01$	$\varepsilon = 0.05$	$\varepsilon = 0.01$	$\varepsilon = 0.05$
AT	8.16	12.61	82.68 (10.13)	99.76 (7.91)
BE	30.61	53.07	284.19 (9.28)	316.05 (5.96)
BG	9.45	15.05	67.60 (7.15)	77.59 (5.16)
CH	2.72	5.33	44.86 (16.50)	48.66 (9.13)
CZ	4.09	9.34	109.32 (26.73)	121.19 (12.98)
DE	672.15	917.10	3512.92 (5.23)	3976.74 (4.34)
DK	23.81	33.15	170.56 (7.16)	198.04 (5.97)
EE	0.03	0.08	5.76 (192.00)	7.24 (90.50)
ES	550.36	624.77	1425.75 (2.59)	1549.28 (2.48)
FI	0.08	0.29	19.18 (239.75)	24.16 (83.31)
FR	313.82	381.75	895.10 (2.85)	978.09 (2.56)
GB	320.28	425.17	1231.19 (3.84)	1359.99 (3.20)
GR	121.57	136.47	274.29 (2.26)	291.17 (2.13)
HR	0.34	0.72	9.70 (28.53)	10.91 (15.15)
HU	0.57	0.90	8.66 (15.19)	9.93 (11.03)
IE	0.02	0.25	48.07 (2403.50)	72.65 (290.60)
IT	563.05	667.90	1533.34 (2.72)	1632.95 (2.44)
LT	0.38	0.83	10.09 (26.55)	11.55 (13.92)
LU	0.48	0.89	8.34 (17.38)	9.37 (10.53)
LV	0.01	0.03	1.24 (124.00)	1.38 (46.00)
NL	27.18	43.93	212.59 (7.82)	243.07 (5.53)
NO	1.03	6.33	24.39 (23.68)	38.55 (6.09)
PL	1.39	2.54	106.32 (76.49)	141.77 (55.81)
PT	44.06	49.35	183.59 (4.17)	228.16 (4.62)
RO	5.53	11.05	119.47 (21.60)	134.11 (12.14)
SE	1.53	2.55	68.93 (45.05)	85.21 (33.42)
SI	0.06	0.66	10.41 (173.50)	11.75 (17.80)
SK	1.98	4.06	27.85 (14.07)	29.99 (7.39)

5. Conclusion

Our work examines the economic value of cooperation between wind and solar producers in the European day-ahead electricity market across 28 countries, using chance-constrained optimization models applied to the EMHIRES generation dataset. Our analysis yields several key insights.

In the Naive setup without storage, cooperation almost uniformly outperforms separate operation. At a relaxed reliability level ($\varepsilon = 0.05$), all countries except Latvia, Norway, Slovenia, and

Slovakia achieve at least a 20% profit gain from cooperation. These four countries have either a PV share below 0.5% or above 98%, which limits the potential for meaningful synergy. In Estonia, Finland, and Ireland, where PV share is less than one percent, Synergy Ratios under the stricter $\varepsilon = 0.01$ requirement are either undefined or highly variable. By contrast, countries such as Finland, Lithuania, and Poland achieve the largest Synergy Ratios — often above a factor of seven and occasionally reaching values near thirty — simply because their PV shares are very small (below 10%), and, thus, provide strong complementarity with wind. These findings confirm that natural negative correlation between wind and solar generation can act as a powerful hedge against delivery risk, though the resulting profits remain volatile when reliability constraints are tight.

In the Storage-Enhanced model (where the battery size is either the installed capacity for each technology, or the sum of these in the joint operation case), 18 out of 28 countries show a clear cooperative benefit, with profit increases of at least 10% and up to 50%. Since storage guarantees strictly positive profits in individual systems, Synergy Ratios are always defined; further, confidence intervals are narrow: lower bounds range from 1.00 to 1.39, and upper bounds from 1.00 to 1.51. This illustrates how storage stabilizes profits and makes outcomes far less sensitive to the reliability threshold. At the same time, the battery storage substitutes for natural balancing in countries where one resource is negligible. Finland, Ireland, Norway, Slovakia, and Slovenia all record ratios close to one, showing that cooperation adds little once storage is available. In contrast, balanced systems such as Belgium, Lithuania, the Netherlands, and Romania sustain Synergy Ratios between 1.3 and 1.5, confirming that cooperation continues to pay off in regions with moderate negative correlations and sufficient PV scale.

The sensitivity analysis with smaller and larger storage capacities reinforces these patterns. When the battery capacity is reduced by 50%, 21 of 28 countries achieve at least a 10% profit gain, with some reaching up to 70%. With a 100% increase, 16 countries show such gains. Here, we see that when the battery size is smaller, the Synergy Ratio is larger but wider in its confidence interval, while with a larger battery size, cooperation profit is smaller but more robust for this metric. The highest values in this setting occur in Belgium, Bulgaria, Lithuania, Romania, and the Netherlands (nearly all are all clustered in the Atlantic and Mediterranean regions), with PV proportions between 9.1% and 56.1%. By contrast, Finland, Ireland, Norway, Slovakia, and Slovenia have Synergy Ratios just above one, reflecting the lack of meaningful contribution from either of the two resources. Together, these results show that storage raises overall profits but redistributes the value of complementarity: it amplifies cooperation in balanced portfolios, while crowding it out in resource-scarce systems.

Overall, our findings suggest a clear policy direction for renewable integration. In regions where wind and solar resources are both significant and moderately negatively correlated—especially in the late afternoon—cooperation among independent producers can deliver stable and economically meaningful gains, particularly when supported by appropriately sized batteries (not larger than

installed capacity). In contrast, where one resource is minimal, policymakers should prioritize expanding renewable capacity before expecting cooperation to yield benefits. More broadly, our results highlight that promoting coordinated bidding of complementary renewables may be a cost-effective alternative to large-scale storage investments.

Finally, beyond our empirical insights, our work demonstrates the versatility of chance-constrained optimization as a framework for evaluating renewable cooperation under uncertainty. By varying the reliability threshold ε, this approach quantifies the trade-off between risk and profit, offering a practical tool for both market design and long-term planning of renewable portfolios in Europe.

CRediT authorship contribution statement

Montree Jaidee: Conceptualization, Methodology, Software, Writing - Original Draft, Review & Editing. **Bismark Singh**: Conceptualization, Methodology, Writing - Original Draft, Review & Editing, Supervision.

Acknowledgement

Montree Jaidee is supported by a scholarship from the Development and Promotion of Science and Technology Talents Project (DPST). Both authors acknowledge the use of the IRIDIS High-Performance Computing Facility at the University of Southampton in completing this work.

References

Aflaki, S., & Netessine, S. (2017). Strategic investment in renewable energy sources: The effect of supply intermittency. *Manufacturing & Service Operations Management*, *19*, 489–507. doi:10.1287/msom.2017.0621.

Atakan, S., Gangammanavar, H., & Sen, S. (2022). Towards a sustainable power grid: Stochastic hierarchical planning for high renewable integration. *European Journal of Operational Research*, *302*, 381–391. doi:10.1016/j.ejor.2021.12.042.

Ferrer-Martí, L., Domenech, B., García-Villoria, A., & Pastor, R. (2013). A MILP model to design hybrid wind–photovoltaic isolated rural electrification projects in developing countries. *European Journal of Operational Research*, *226*, 293–300. doi:10.1016/j.ejor.2012.11.018.

Gaur, V., & Seshadri, S. (2005). Hedging inventory risk through market instruments. *Manufacturing & Service Operations Management*, *7*, 103–120. doi:10.1287/msom.1040.0061.

Glenk, G., & Reichelstein, S. (2020). Synergistic value in vertically integrated power-to-gas energy systems. *Production and Operations Management*, *29*, 526–546. doi:10.1111/poms.13116.

Golari, M., Fan, N., & Jin, T. (2017). Multistage stochastic optimization for production-inventory planning with intermittent renewable energy. *Production and Operations Management*, *26*, 409–425. doi:10.1111/poms.12657.

Gonzalez Aparicio, I., Huld, T., Careri, F., Monforti Ferrario, F., & Zucker, A. (2017). Solar hourly generation time series at country, NUTS 1, NUTS 2 level and bidding zones. European Commission, Joint Research Centre (JRC). [Dataset] http://data.europa.eu/89h/jrc-emhires-solar-generation-time-series.

Gonzalez Aparicio, I., Zucker, A., Careri, F., Monforti Ferrario, F., Huld, T., & Badger, J. (2016). Wind hourly generation time series at country, NUTS 1, NUTS 2 level and bidding zones. European Commission, Joint Research Centre (JRC). [Dataset] http://data.europa.eu/89h/jrc-emhires-wind-generation-time-series.

Hu, S., Souza, G. C., Ferguson, M. E., & Wang, W. (2015). Capacity investment in renewable energy technology with supply intermittency: Data granularity matters! *Manufacturing & Service Operations Management*, *17*, 480–494. doi:10.1287/msom.2015.0536.

Jordan, W. C., & Graves, S. C. (1995). Principles on the benefits of manufacturing process flexibility. *Management Science*, *41*, 577–594. doi:10.1287/mnsc.41.4.577.

Kaut, M., Vaagen, H., & Wallace, S. W. (2021). The combined impact of stochastic and correlated activity durations and design uncertainty on project plans. *International Journal of Production Economics*, *233*, 108015. doi:10.1016/j.ijpe.2020.108015.

Li, C., Ge, X., Zheng, Y., Xu, C., Ren, Y., Song, C., & Yang, C. (2013). Techno-economic feasibility study of autonomous hybrid wind/PV/battery power system for a household in Urumqi, China. *Energy*, *55*, 263–272. doi:10.1016/j.energy.2013.03.084.

Nandi, S. K., & Ghosh, H. R. (2010). Prospect of wind–PV-battery hybrid power system as an alternative to grid extension in Bangladesh. *Energy*, *35*, 3040–3047. doi:10.1016/j.energy.2010.03.044.

Piel, J.-H., Hamann, J. F., Koukal, A., & Breitner, M. H. (2017). Promoting the system integration of renewable energies: Toward a decision support system for incentivizing spatially diversified deployment. *Journal of Management Information Systems*, *34*, 994–1022. doi:10.1080/07421222.2017.1394044.

Salman, M., Kashif, S. A. R., Fakhar, M. S., Rasool, A., & Hussen, A. S. (2025). Optimizing power generation in a hybrid solar wind energy system using a DFIG-based control approach. *Scientific Reports*, *15*. doi:10.1038/s41598-025-95248-8.

Singh, B., & Knueven, B. (2021). Lagrangian relaxation based heuristics for a chance-constrained optimization model of a hybrid solar-battery storage system. *Journal of Global Optimization*, *80*, 965–989. doi:10.1007/s10898-021-01041-y.

Singh, B., Morton, D. P., & Santoso, S. (2018). An adaptive model with joint chance constraints for a hybrid wind-conventional generator system. *Computational Management Science*, *15*, 563–582. doi:10.1007/s10287-018-0309-x.

Singh, B., & Pozo, D. (2019). A guide to solar power forecasting using ARMA models. In *2019 IEEE PES Innovative Smart Grid Technologies Europe (ISGT-Europe)* (pp. 1–4). IEEE. doi:10.1109/isgteurope.2019.8905430.

Sunar, N., & Birge, J. R. (2019). Strategic commitment to a production schedule with uncertain supply and demand: Renewable energy in day-ahead electricity markets. *Management Science*, *65*, 714–734. doi:10.1287/mnsc.2017.2961.

Wolff, M., Becker, T., & Walther, G. (2023). Long-term design and analysis of renewable fuel supply chains — an integrated approach considering seasonal resource availability. *European Journal of Operational Research*, *304*, 745–762. doi:10.1016/j.ejor.2022.04.001.